Freshwater input and vertical mixing in the Canada Basin's seasonal halocline: 1975 versus 2006-2012

Erica Rosenblum*

Centre for Earth Observation Science, University of Manitoba, Winnipeg, Manitoba, Canada

Department of Atmospheric Science, McGill University, Montreal, Quebec, Canada

Julienne Stroeve

Centre for Earth Observation Science, University of Manitoba, Winnipeg, Manitoba, Canada

Centre for Polar Observation and Modelling, University College London, Earth Sciences, London, United Kingdom

National Snow and Ice Data Center, Cooperative Institute for Research in Environmental Sciences, University of Colorado, Boulder, CO, USA

Sarah T. Gille

Scripps Institution of Oceanography, University of California San Diego, La Jolla, California, USA

L. Bruno Tremblay

Department of Atmospheric Science, McGill University, Montreal, Quebec, Canada

Camille Lique

University of Brest, CNRS, IRD, Ifremer, Laboratoire d'Océanographie Physique et Spatiale (LOPS), IUEM, Brest, France

Robert Fajber

Department of Physics, University of Toronto, Toronto, Ontario, Canada

Ryan Galley

Department of Environment and Geography, University of Manitoba, Winnipeg, Manitoba, Canada

David G. Barber

Centre for Earth Observation Science, University of Manitoba, Winnipeg, Manitoba, Canada

Thiago Loureiro

Toronto, Ontario, Canada

Jennifer V. Lukovich

Centre for Earth Observation Science, University of Manitoba, Winnipeg, Manitoba, Canada

* *Corresponding author address:* Erica Rosenblum, Centre for Earth Observation Science, University of Manitoba, Winnipeg, Manitoba, Canada.

E-mail: erica.rosenblum@umanitoba.ca

ABSTRACT

The seasonal halocline impacts the exchange of heat, energy, and nutrients between the surface and the deeper ocean, and it is changing in response to Arctic sea ice melt over the past several decades. Here, we assess seasonal halocline formation in 1975 and 2006-2012 by comparing daily, May to September, below-ice salinity profiles collected in the Canada Basin. We evaluate differences between the two time periods using a one-dimensional (1D) bulk model to quantify differences in freshwater input and vertical mixing. The 1D model metrics indicate that two separate factors contribute similarly to stronger stratification in 2006-2012 than in 1975: (1) larger surface freshwater input and (2) less vertical mixing of that freshwater. The first factor is mainly important in August-September, consistent with a longer melt season in recent years. The second factor is mainly important from June until mid-August, when similar levels of freshwater input in 1975 and 2006-2012 are mixed over a different depth range, resulting in different stratification. These results imply that decadal changes to ice-ocean dynamics, in addition to freshwater input, significantly contribute to the stronger seasonal stratification in 2006-2012 than in 1975. The findings highlight the need for near-surface process studies to elucidate the roles of lateral processes and ice-ocean momentum exchange on vertical mixing.

1. Introduction

The surface waters of the Arctic Ocean have changed dramatically over the past several decades as a result of the diminishing sea ice cover that once shielded much of the ocean from wind and sunlight across all seasons (Perovich 2011; McLaughlin et al. 2011; Stroeve and Notz 2018; Polyakov et al. 2020), and this has important consequences for the exchange of heat and nutrients between the surface and deeper ocean (McLaughlin et al. 2011; Carmack et al. 2015; Timmermans and Marshall 2020; Brown et al. 2020). Changes in Arctic sea ice conditions are generally thought to either strengthen or weaken the underlying upper-ocean stratification depending on the competing effects of freshwater input and of vertical mixing (Peralta-Ferriz and Woodgate 2015; Lique 2015; Nummelin et al. 2015; Davis et al. 2016). A now warmer atmosphere and ocean delays ice freeze-up, reduces winter ice growth, and can melt more sea ice each spring and summer, potentially releasing more fresh, buoyant meltwater to the surface (Stroeve et al.; Carmack et al. 2016) that can stabilize the upper ocean. Conversely, the wind acts on a now more mobile ice pack (Rampal et al. 2009; Galley et al. 2013; Kwok et al. 2013; Brown et al. 2020), potentially generating greater shear that stirs and mixes the underlying ocean, that can reduce the stability of the upper ocean (Lemke and Manley 1984; Polyakov et al. 2020). Increased stratification has been documented in recent decades in many regions of the Arctic, but the exact link between freshwater input and upper-ocean vertical mixing remains an open question.

We examine this question by comparing the seasonal evolution of the upper ocean below sea ice during two time periods that are separated by approximately three decades, and that are associated with distinctly different sea ice conditions. The datasets come from the 1975 Arctic Ice Dynamics Joint Experiment (AIDJEX) program (Untersteiner et al. 2007) and from the 2004-present Ice-Tethered Profiler (ITP) instrumentation system (Krishfield et al. 2008). Compared to the 1975

AIDJEX dataset, the ITP dataset is associated with lower sea ice concentration (Fig. 1), has less multi-year sea ice area and volume (Wadhams 2012; Kwok 2018), and is made up of smaller ice floes (Hutchings and Faber 2018) that are both thinner (Kwok and Rothrock 2009; Kwok 2018) and less deformed, with shallower ridges (Wadhams 2012; Hutchings and Faber 2018; Kwok 2018).

Both the ITP and AIDJEX data were collected in the Canada Basin (Fig. 1), where the upper-ocean hydrography evolves seasonally in response to changes in sea ice (McPhee and Smith 1976; Morison and Smith 1981; Lemke and Manley 1984; Jackson et al. 2010; Toole et al. 2010; Peralta-Ferriz and Woodgate 2015), river runoff (Macdonald et al. 1999; Yamamoto-Kawai et al. 2009), and Ekman dynamics in the Beaufort Gyre (Proshutinsky et al. 2009; Carmack et al. 2016; Meneghello et al. 2018). In the spring and summer, freshwater flux from snow and sea ice melt causes the surface mixed layer to freshen and shoal, forming a seasonal halocline. The predominant, clockwise atmospheric circulation (Beaufort High) drives convergent Ekman pumping in the Beaufort Gyre most noticeably in the fall, causing low salinity surface water to converge and the halocline to deepen within the basin (Reed and Kunkel 1960; Gudkovich 1961; Hunkins and Whitehead 1992; Proshutinsky et al. 2009; Newton et al. 2006; Jackson et al. 2010; McLaughlin and Carmack 2010; Meneghello et al. 2018). In the winter, sea ice formation results in brine rejection, which increases the surface water salinity and causes convectively-driven mixed-layer deepening that erodes the seasonal halocline.

Comparisons of single representative profiles from ITP and AIDJEX data that were collected in roughly the same location indicate a trend toward fresher surface waters, shallower mixed layers, and a more stably stratified upper ocean (Toole et al. 2010; McPhee 2012), similar to the comparison of AIDJEX and 1997 Surface HEat Budget of the Arctic (SHEBA) data (McPhee et al. 1998). June–September and November–May seasonal averages of hydrographic data across the Arctic during 1979-2012, which did not include ITP or AIDJEX data, confirmed statistically significant ∼30-year trends toward a more stably stratified upper ocean with shallower and fresher mixed layers in the Canada Basin (Peralta-Ferriz and Woodgate 2015). Decadal changes to the surface waters were primarily attributed to increased freshwater input from ice melt, river run-off, and precipitation. This freshwater has collected toward the center of an intensified anticyclonic (convergent) Beaufort Gyre (Macdonald et al. 1999; Proshutinsky et al. 2009; Jackson et al. 2010; McLaughlin and Carmack 2010; Steele et al. 2011; Peralta-Ferriz and Woodgate 2015). However, the seasonality of the freshwater input, the vertical extent of wind-driven mixing, and upper-ocean stratification was not addressed in these previous studies.

In this study, we compare seasonal processes of the upper ocean by focusing on the evolving time series from May to September in the 2006-2012 ITP data and 1975 AIDJEX data. This seasonal analysis differs from previous studies that compared two single profiles (Toole et al. 2010; McPhee et al. 1998), two 20-day average profiles (McPhee 2012), or used four and seven month averages (Peralta-Ferriz and Woodgate 2015). We interpret the results using a simple one-dimensional bulk model of seasonal halocline formation that allows for the comparison of the ITP and AIDJEX data in terms of seasonal freshwater input and vertical mixing. The datasets used for this study are presented in Section 2, and the one-dimensional model is presented in Section 3. In Section 4, we present results comparing the ITP and AIDJEX hydrographic data in conjunction with the one-dimensional model. We discuss mechanisms that could explain changes to the relationship between freshwater input, vertical mixing, and stratification during the two time periods in Section 5 and summarize our results in Section 6.

2. Data

This study addresses spring-to-summer halocline formation associated with two distinctly different time periods and sea ice regimes. To this end, we use May–September data from the AIDJEX and ITP programs.

A major component of the AIDJEX program consisted of four occupied, drifting ice camps where oceanographic data were collected for approximately one year between May 1975 and April 1976 (Table 1). Salinity and temperature profiles between depths of 5 m and 750 m were measured daily at each camp, with a vertical resolution of 1–2 m, using a Plessey model 9040 conductivity, temperature, depth measurement system, resulting in 1279 vertical profiles. See Maykut and McPhee (1995) for a full description of the data used in this analysis.

The ITP instrument system records temperature and salinity profiles with a vertical resolution of 25 cm throughout the Arctic. The system consists of a series of surface buoys, frozen into drifting ice floes, connected to 800-m-long wires. CTD profilers move up and down the wires collecting data approximately 2-3 times per day. We use quality-controlled data, identified as level 3 in the ITP data archives, which have 1 m vertical resolution and were available for 2004-2012 at the time of the analysis. We examine all available level-3 processed data within the Canada Basin, which we define as the region bounded by 72°N, 80°N, 130°W, and 155°W (similar to the region defined by Peralta-Ferriz and Woodgate (2015); dashed lines, Fig. 1). Further, we select only ITPs that have data starting in May of a given year, similar to the data available from the AIDJEX ice camps. Lastly, profiles were removed if the shallowest observed value was deeper than 10 meters (following Jackson et al. 2010), which helps to account for the fact that ITPs often start sampling too far from the surface to accurately measure the summer mixed layer.

In total, 517 AIDJEX profiles collected in 1975 from 4 ice camps and 2892 ITP profiles collected between 2006-2012 from 12 different ITPs satisfied these criteria (Table 1), with average shallowest measurements of ~ 6 m and ~ 7 m, respectively. All profiles were linearly interpolated onto a common 1-m vertical grid. Ice thickness measurements are not available for all ITP profiles or AIDJEX ice camps. For both datasets, we therefore assume an ice–ocean interface at 3 m, a climatological multi-year sea ice thickness in the Canada Basin, and keep the salinity and temperature constant from the shallowest measurements of each profile to $z = -3$ m, with the z-axis defined as positive up. We discuss the sensitivity of our results to missing near-surface data in Section 5.

To estimate the freshwater input from sea ice melt, we also examine 1979-2018 sea ice volume estimates provided by the Pan-arctic Ice Ocean Modeling and Assimilation System (Schweiger et al. 2011). The PIOMAS sea ice volume was regridded to the 25 km Equal-Area Scalable Earth (EASE) grid and averaged over the Canada Basin (bounded by 72°N, 80°N, 130°W, and 155°W, as in the hydrographic data).

To qualitatively compare the sea ice conditions associated with the AIDJEX and ITP datasets, we examine 1975 and 2006-2012 sea ice concentrations. Daily 2006-2012 sea ice concentration observations are provided by Passive Microwave satellite data, Version 1 (Cavalieri et al. 1996), which combines data from the Defense Meteorological Satellite Program Special Sensor Microwave/Imager (DMSP SSM/I, 2006-2007) and the Special Sensor Microwave Imager/Sounder (SSMI/S, 2007-2012). Sea ice concentration data are co-located to each ITP observation. We note that low sea ice concentration from the passive microwave data can imply either low ice concentration or surface melt ponds (e.g., Kern et al. 2016). Since the AIDJEX data were collected in 1975, before the satellite data were available, we use the Canadian Ice Service digital archive (CISDA) chart data for the western Arctic region to determine the temporal evolution of sea ice concentration during that year in the Canada basin region (Tivy et al. 2011). Gridded datasets for each CISDA chart in June-September 1975 were analyzed to provide a weekly regional mean sea ice concentration.

3. One-Dimensional Framework

One-dimensional (1D) ice-ocean models are used to provide a framework for interpreting observed seasonal mixed-layer evolution (Morison and Smith 1981; Lemke and Manley 1984; Lemke 1987; Toole et al. 2010; Petty et al. 2013; Tsamados et al. 2015). Here, we model seasonal halocline formation starting from a homogeneous winter mixed layer in an idealized system (Fig. 2), building off of conceptual models used to estimate freshwater input, vertical mixing, and upper-ocean stratification from hydrographic data in previous studies (Simpson et al. 1978; Peralta-Ferriz and Woodgate 2015; Randelhoff et al. 2017). This idealized model omits a range of processes associated with horizontal advection and ice formation; the impact of these will be considered in Section 4.

a. Model Equations

We consider a closed, 1D ice-ocean system with an ocean of depth L that only evolves in response to thermodynamic sea ice melt and vertical mixing with the following initial conditions ($t = t_0$): a well-mixed ocean, with vertically uniform salinity (S_0) and potential density (ρ_0), and sea ice with constant salinity (S_{ice}) and density (ρ_{ice}). If melt water is vertically mixed to some depth, Z_{fw}, then the salinity and density below this depth remains fixed at S_0 and ρ_0 (i.e., $S(z) = S_0$ and $\rho(z) = \rho_0$ for $z \leq Z_{fw}$, where z and Z_{fw} are both negative). The conservation of salt and mass for time $t > t_0$ can be written as:

$$\begin{aligned} \int_{Z_{fw}(t)}^{Z_{ice}} \rho(t,z)S(t,z)\cdot dz - \rho_0 S_0(Z_{ice} - Z_{fw}(t)) &= \rho_{ice}S_{ice}h_{melt}(t) \quad (1) \\ \int_{Z_{fw}(t)}^{Z_{ice}} \rho(t,z)\cdot dz - \rho_0(Z_{ice} - Z_{fw}(t)) &= \rho_{ice}h_{melt}(t), \quad (2) \end{aligned}$$

where Z_{ice} is the ice draft, h_{melt} is the change in sea ice thickness from melt, $\rho(t,z)$ and $S(t,z)$ are the ocean potential density and salinity, respectively. The above expressions, therefore, represent the change in mass and salt in the ocean (left-hand side) in response to sea ice melt (right-hand side). These equations can be algebraically combined to estimate the sea ice melt necessary to explain the transition from the initial, well-mixed ocean (S_0, ρ_0) to the subsequent ocean profile that includes vertically mixed meltwater ($S(t,z)$, $\rho(t,z)$) at any time $t > t_0$:

$$h_{melt}(t) = \int_{Z_{fw}(t)}^{Z_{ice}} \frac{\rho(t,z)(S(t,z) - S_0)}{\rho_{ice}(S_{ice} - S_0)} \cdot dz. \quad (3)$$

Alternatively, h_{melt} can be written in terms of pure freshwater, rather than ice melt, by replacing S_{ice} and ρ_{ice} with values for freshwater ($S_{FW} = 0$ and ρ_{FW}). Further, if we assume that the density of freshwater and salt water are approximately equal, equation (3) becomes: $\mathrm{sFWC}(t) = \int_{Z_{fw}(t)}^{Z_{ice}} (S_0 - S(t,z))/S_0 \cdot dz$, similar to the expression for freshwater content (FWC) used in numerous studies. However, FWC incorporates a reference salinity, set to the Arctic Ocean mean salinity of 34.8 psu (Carmack et al. 2016), while sFWC is referenced to the initial conditions, S_0. This difference implies that h_{melt} and sFWC reflect the seasonal near-surface freshwater content. This approach is similar to previous studies that estimated sea ice melt from mixed-layer salinity evolution (Lemke and Manley 1984; Peralta-Ferriz and Woodgate 2015), but here the depth range is set by Z_{fw} and Z_{ice} rather than a mixed-layer depth criterion. That is, we estimate the freshwater input from sea ice melt over a well-defined volume, which avoids errors that can arise when using a reference salinity (Schauer and Losch 2019).

We will also use the vertically integrated change in salinity relative to S_0, sometimes referred to as the “salt deficit” or “buoyancy deficit” (Martinson 1990; Martinson and Iannuzzi 1998; Randelhoff et al. 2017):

$$\Phi(t) = \int_{Z_{fw}(t)}^{Z_{ice}} S_0 - S(t,z) \cdot dz. \tag{4}$$

Φ is approximately linearly related to h_{ice} and, therefore, also provides a bulk estimate of the cumulative amount of freshwater input at any time $t > t_0$.

Different salinity profiles are possible in response to the same amount of ice melt, depending on how the melt water is vertically spread or mixed through the water column (Fig. 2). For example, if the melt water were concentrated close to the surface (less vertical mixing, shallow Z_{fw}), this would result in more surface freshening and a more stably stratified water column with a lower potential energy (Fig. 2; left side). Alternatively, if the melt water were spread over a larger depth range (more vertical mixing, deep Z_{fw}), this would result in less surface freshening and a less stably stratified water column with a higher potential energy (Fig. 2; right side).

To quantify this effect, we will consider two bulk metrics of stratification. First, we define the surface freshening at any time $t > t_0$ as the surface salinity anomaly relative to the initial condition:

$$\mathbb{S}(t) = S(t, Z_{ice}) - S_0. \tag{5}$$

Second, we consider the potential energy relative to the mixed state (Simpson and Hunter 1974; Simpson et al. 1978):

$$\mathbb{W}(t) \equiv \int_{H}^{Z_{ice}} \left(\rho(t,z) - \langle \rho(t) \rangle\right) g\, z \cdot dz, \tag{6}$$

where

$$\langle \rho(t) \rangle = \frac{1}{Z_{ice} - H} \int_{H}^{Z_{ice}} \rho(t,z) \cdot dz. \tag{7}$$

In equation (6), the first term represents the total potential energy at time t, and the second term represents the potential energy that the fluid would have if it were in a well-mixed (homogenized) state within the top $|H|$ meters, with uniform density $\langle\rho(t)\rangle$ (i.e., the state in which the potential energy is maximized). $\mathbb{W} = 0$ for a well-mixed system and $\mathbb{W} < 0$ for a stably stratified system. Considering the conservation of energy (neglecting dissipation), $|\mathbb{W}|$ provides a measure of the work or kinetic energy input needed to completely mix the water column to any depth H. We note that $\mathbb{W}$ differs from the available potential energy (APE), which is a measure of the change in potential energy that would occur if the fluid were adiabatically re-arranged to minimize the potential energy (Lorenz 1955), rather than diapycnally mixed to maximize the potential energy.

b. Separating freshwater input and vertical mixing

We seek bulk representations of $\mathbb{S}$ and $\mathbb{W}$ to directly compare the 1975 AIDJEX data and 2006-2012 ITP data in terms of changes to (1) the seasonal freshwater input and (2) vertical mixing. That is, for any time $t > t_0$, we seek:

$$\delta\mathbb{S}(t) = f(\delta\Phi(t), \delta D(t)) \tag{8}$$

$$\delta\mathbb{W}(t) = f(\delta\Phi(t), \delta D(t)), \tag{9}$$

where δ indicates the difference between ITP and AIDJEX data, and D is a bulk indicator of the vertical mixing, where we define larger and smaller mixing as mixing that leads to a deeper or shallower seasonal halocline.

We choose the equivalent mixed-layer depth, an integral quantity that is closely related to the vertical extent of wind-driven mixing (Randelhoff et al. 2017):

$$D(t) = \frac{\Phi(t)}{\mathbb{S}(t)}, \tag{10}$$

where $D + Z_{ice}$ indicates the depth of the halocline if the meltwater were completely mixed (i.e., if the salinity were homogenized), implying that the salinity profile would have a two-layer form and $D + Z_{ice} = Z_{fw}$:

$$S_{bulk}(t,z) = \begin{cases} S_0 + \Phi(t)/D(t) & D(t) + Z_{ice} \leq z \leq Z_{ice} \\ S_0 & z < D(t) + Z_{ice} \end{cases} \tag{11}$$

(see Fig. 2 for an illustration of this 2-layer profile).

Next, we seek a bulk estimate of the potential energy anomaly ($\mathbb{W}$) associated with the 2-layer system. We first assume that the density varies linearly with salinity ($\rho_{bulk}(t,z) - \rho_0 = \beta(S_{bulk}(t,z) - S_0)$), implying that the 2-layer potential density profile (ρ_{bulk}) can be written as:

$$\rho_{bulk}(t,z) = \begin{cases} \rho_0 + \beta\Phi(t)/D(t) & D(t) + Z_{ice} \leq z \leq Z_{ice} \\ \rho_0 & z < D(t) + Z_{ice}, \end{cases} \tag{12}$$

where β is the haline contraction coefficient.

Applying (12) to (6) and (7), we can write an expression for $\mathbb{W}$ associated with the 2-layer system:

$$\mathbb{W}_{bulk}(t) = \int_{H-Z_{ice}}^{0} (\rho_{bulk}(t,z') - \langle\rho_{bulk}(t)\rangle) g z' dz' \tag{13}$$

and

$$\langle\rho_{bulk}(t)\rangle = \frac{1}{H - Z_{ice}} \int_{H-Z_{ice}}^{0} \rho_{bulk}(t,z') dz' \tag{14}$$

where we have applied a change of variables $z' = z - Z_{ice}$. The above expression for $\mathbb{W}_{bulk}$ can then be reduced to:

$$\mathbb{W}_{bulk}(t) = \frac{\beta\Phi(t)g}{2}(H - D(t) - Z_{ice}), \tag{15}$$

for any time $t \geq t_0$.

The bulk representation of the surface freshening ($\mathbb{S}$) associated with this 2-layer system for any time $t \geq t_0$ is:

$$\mathbb{S}_{bulk}(t) = \frac{\Phi(t)}{D(t)}, \tag{16}$$

following equation (10). $\mathbb{S}_{bulk}$, therefore, indicates the salt content changes within the mixed layer D.

Two factors determine $\mathbb{S}_{bulk}$ and $\mathbb{W}_{bulk}$: (1) the amount of freshwater input (related to Φ) and (2) the concentration or dilution of that freshwater toward the surface by vertical mixing (related to D). We can, therefore, estimate how each factor contributes to $\delta\mathbb{S}$ and $\delta\mathbb{W}$ (see eq. (8)-(9)) by writing $\mathbb{S}_{bulk}$ and $\mathbb{W}_{bulk}$ derived from 2006-2012 ITP data in terms of the changes relative to the 1975 AIDJEX data:

$$\mathbb{S}_{ITP}(t) = \frac{\Phi_{AJX}(t)+\delta\Phi(t)}{D_{AJX}(t)+\delta D(t)}, \tag{17}$$

$$\mathbb{W}_{ITP}(t) = \frac{\beta g}{2}(\Phi_{AJX}(t)+\delta\Phi(t))\cdot(H-Z_{ice}-(D_{AJX}(t)+\delta D(t))), \tag{18}$$

where ITP indicates that the value is derived from ITP data, AJX indicates that the value is derived from AIDJEX data, and δ is the difference between ITP and AIDJEX data ($\delta X = X_{ITP} - X_{AJX}$).

The difference between $\mathbb{S}_{bulk}$ in 1975 and 2006-2012 ($\delta\mathbb{S} = \mathbb{S}_{ITP} - \mathbb{S}_{AJX}$) can then be re-written algebraically to isolate the relative contributions of $\delta\Phi$ and δD on $\delta\mathbb{S}$:

$$\delta\mathbb{S}(t) = \underbrace{\frac{\delta\Phi(t)}{D_{AJX}(t)}}_{\substack{\text{changes to}\\ \text{freshwater}}} - \underbrace{\frac{\Phi_{AJX}(t)\delta D(t)}{D_{AJX}(t)(D_{AJX}(t)+\delta D(t))}}_{\substack{\text{changes to}\\ \text{vertical mixing}}} - \underbrace{\frac{\delta\Phi(t)\delta D(t)}{D_{AJX}(t)(D_{AJX}(t)+\delta D(t))}}_{\text{coupled term}}. \tag{19}$$

Similarly, the difference between $\mathbb{W}_{bulk}$ in 1975 and 2006-2012 ($\delta\mathbb{W} = \mathbb{W}_{ITP} - \mathbb{W}_{AJX}$) can be written as:

$$\delta\mathbb{W}(t) = \frac{\beta g}{2}(\underbrace{(H-Z_{ice}-D_{\mathrm{AJX}}(t))\delta\Phi(t)}_{\substack{\text{changes to}\\ \text{freshwater}}} - \underbrace{\Phi_{\mathrm{AJX}}(t)\delta D(t)}_{\substack{\text{changes to}\\ \text{vertical mixing}}} - \underbrace{\delta\Phi(t)\delta D(t)}_{\text{coupled term}}) \tag{20}$$

(see Supporting Information for full derivation).

The three terms on the right-hand sides of (19) and (20) are estimates of the decadal changes to the stratification associated with (1) changes related to the amount of freshwater input ($\delta\Phi$), holding the vertical mixing to AIDJEX values (D_{AJX}); (2) changes to the vertical mixing (δD), holding the amount of freshwater input equal to AIDJEX values (Φ_{AJX}); and (3) the contribution from the two terms coupled together.

We note that $\mathbb{S}_{bulk}$ and $\mathbb{W}_{bulk}$ have a similar dependence on Φ and D. However, $\mathbb{S}$ depends on the initial condition, S_0, but not a chosen depth range, H, while $\mathbb{W}$ depends on H but not S_0. We, therefore, use the observations to explore both of these expressions.

4. Results

The observations indicate that the surface is $\sim$ 2-4 g/kg fresher in 2006-2012 than in 1975, yet both time periods have a similar seasonal evolution (Fig. 3). At the beginning of May, both datasets indicate mixed layers that are relatively deep (thick black lines, Fig. 3a). As spring progresses, the surface freshens and the seasonal halocline forms (dashed black lines, Fig. 3a,b). Toward the end of summer, sea ice forms, the surface becomes progressively saltier, and the mixed layer deepens, eroding the seasonal halocline (compare dashed and thick black lines, Fig. 3b). Compared to 1975, 2006-2012 appears to have more seasonal freshwater stored closer to the surface, resulting in more seasonal surface freshening and a more stably stratified upper ocean for a longer time period. Qualitatively, this is consistent with the previous studies described in Section 1.

To compare the seasonal evolution of the upper-ocean during 1975 and 2006-2012 using the 1D framework, we set S_0 equal to the May-average surface salinity ($S(Z_{ice})$) measured by the same ITP or AIDJEX ice camp during the same year and we set $H = 30$ m. That is, we examine the seasonal freshwater input (Φ, h_{melt}), vertical mixing (Z_{fw}, D), and the surface freshening ($\mathbb{S}$) relative to the May average, which marks the beginning of the melt season measured by a given ITP or AIDJEX ice camp. We examine $\mathbb{W}$ over the top 30 meters, which corresponds to $\mathbb{W} \sim 0$ in May 1975 and 2006-2012 (see Section 4a), similar to the initial conditions of the 1D framework.

We present results based on alternative values of H and S_0 in the Supporting Information. All other constants are given in Table 2.

Figure 4 shows an example of how various quantities presented in Section 3 are computed for a single profile using observations from one AIDJEX ice camp (Fig. 4; left side) and one ITP (Fig. 4; right side). The freshwater input, indicated by h_{melt} and Φ (Fig. 4c-d), reflects any process that drives changes to the upper-ocean salinity, including sea ice melt, river runoff, precipitation, or advection, although previous studies have demonstrated that the majority of the seasonal freshwater input during the melt season is derived from sea ice melt (e.g., Lemke and Manley 1984; Peralta-Ferriz and Woodgate 2015). Vertical mixing, indicated by Z_{fw} and D (Fig. 4e-f), reflects any process that vertically spreads that freshwater.

a. Validation

To test the validity of our approach, we compare the seasonal freshwater input in terms of the equivalent ice melt (h_{melt}), derived from hydrographic data, to the effective ice thickness change relative to May of each year between 1979-2018 using PIOMAS. We compute h_{melt} associated with each profile in 1975 and 2006-2012. The seasonal evolution of h_{melt} and the monthly ice thickness relative to May are shown in Figure 5. Both estimates indicate sea ice melt through August. In 1975, h_{melt} begins to decrease in early September in response to sea ice formation and entrainment. In 2006-2012, h_{melt} continues to increase through September in response to a later freeze up (Fig. 5a). We find similar results using different definitions of S_0 (Fig. S1).

We find good agreement between the PIOMAS seasonal ice thickness changes and the estimated sea ice melt using oceanographic observations during summer, consistent with previous studies. By the end of August, we find h_{melt} ~0.5-1 m in 1975 and h_{melt} ~1-2 m in 2006-2012, consistent with estimated sea ice melt during similar time periods using hydrographic data (Lemke and

Manley 1984; Peralta-Ferriz and Woodgate 2015) and ice mass balance buoys (e.g., Perovich and Richter-Menge 2015). The consistency of these findings provides indirect evidence that h_{melt} is a reasonable estimate of the seasonal freshwater input. We note that in June, some data points indicate $h_{melt} < 0$. For the remainder of the analysis, we only consider profiles with positive values of h_{melt}.

Using each observed profile, we compare the potential energy anomaly over the top 30 m ($\mathbb{W}$) to the associated two-layer estimate ($\mathbb{W}_{bulk}$). The seasonal evolution of each of these values in the 1975 AIDJEX and 2006-2012 ITP datasets is shown in Figure 6. We find a clear agreement between the observations and the two-layer estimates. First, both $|\mathbb{W}|$ and $|\mathbb{W}_{bulk}|$ indicate that the seasonal halocline forms in late June of 1975 and 2006-2012, but is more stably stratified for a longer period of time in 2006-2012. Second, both $|\mathbb{W}|$ and $|\mathbb{W}_{bulk}|$ are up to five times larger in 2006-2012 than in 1975, implying that five times more energy would be required to deepen the mixed layer to 30 meters. The similarities between $\mathbb{W}$ and $\mathbb{W}_{bulk}$ indicate that the 2-layer simplifications represent the majority of the key features necessary to explain the differences between the upper-ocean seasonal evolution in 1975 and 2006-2012.

The equivalent mixed-layer depth (D) and the associated surface freshening ($\mathbb{S}$) in 1975 and 2006-2012 are shown in Figure 7. These metrics indicate a number of differences between the ITP and AIDJEX datasets that are consistent with previously documented decadal trends in the Canada Basin. Specifically, Peralta-Ferriz and Woodgate (2015) found statistically significant trends of mixed-layer freshening (0.11 psu/yr) and mixed-layer shoaling (0.33 m/yr) during June–September in regions of the Canada Basin with high sea ice concentration (>15%). These rates of change would imply an average change of 3.7 psu and 11.2 m over 34 years, similar to the 3.1 g/kg and 14.5 m difference in the surface salinity ($\mathbb{S} + S_0$) and the equivalent mixed-layer depth (D) between the 1975 AIDJEX data and the 2006-2012 ITP data over the same months.

Overall, these findings suggest that a comparison of the ITP and AIDJEX datasets, in conjunction with the one-dimensional framework presented in Section 3, yields results that are consistent with Peralta-Ferriz and Woodgate (2015) using seasonal averages.

b. 1975 vs 2006-2012

The relationship between estimates of freshwater input from ice melt and other freshwater sources (h_{melt}), vertical mixing (D), and upper-ocean stratification ($\mathbb{S}$,$\mathbb{W}$) is shown in Figure 8, using every June-September profile in 1975 and 2006-2012. During each time period, we find that the parameters exhibit relationships that are qualitatively consistent with a 1D system, where surface fluxes that result in a more buoyant surface layer cause a more stable stratification that inhibits vertical mixing (Turner 1967; Kraus and Turner 1967; Lemke and Manley 1984; Lemke 1987). That is, profiles with more freshwater input (larger h_{melt}) are associated with less vertical mixing (smaller $|D|$) and a more stably stratified upper-ocean (large $|\mathbb{S}|$,$|\mathbb{W}|$).

Considering differences between 1975 and 2006-2012, we find that there are more profiles in 2006-2012 with large values of h_{melt} and hence small values of $|D|$ and large values of $|\mathbb{S}|$ and $|\mathbb{W}|$, as in a 1D system. However, we also consistently find profiles with the same amount of freshwater (h_{melt}) in both time periods but with the freshwater concentrated closer to the surface (smaller $|D|$) in 2006-2012 than in 1975 (Fig. 8a). These differences in $|D|$ are also associated with a more stable stratification (large $|\mathbb{S}|$,$|\mathbb{W}|$; Fig. 8b-c). That is, there are two separate factors causing the more stable stratification in 2006-2012 than in 1975: (1) more freshwater input (larger h_{melt}), which mainly occurs in August and September, and (2) less vertical mixing (smaller $|D|$), which mainly occurs in June and July (Fig. 8; compare top and bottom panels).

We find similar results when examining the relationship between $\delta\mathbb{S}$, $\delta\mathbb{W}$, and δh_{melt} during each 5-day period (Fig. 9); 5-day periods with similar levels of freshwater input in 1975 and

2006-2012 ($\delta h_{melt} \sim 0$) have different stratification ($|\delta \mathbb{S}| > 0$, $|\delta \mathbb{W}| > 0$) from June until mid-August. The largest difference between the two time periods occurs from mid-August through September, coinciding with the largest values of δh_{melt}. Similar results are found using different definitions of H (Fig. S2), though larger values of H extend into the wither halocline and therefore incorporate interannual variations within the winter halocline (e.g., Fig. 3).

We can use the 1D framework (Section 3a) to estimate the relative importance of each of these factors in setting the more stable stratification in 2006-2012 than in 1975. Figure 10b-c shows the 5-day average bulk estimates of the upper-ocean stratification ($\mathbb{S}_{bulk}$, $\mathbb{W}_{bulk}$) in 1975 (blue line) and 2006-2012 (red line). For each 5-day period, we compute the difference between 1975 and 2006-2012 ($\delta \mathbb{S}, \delta \mathbb{W}$) in terms of (1) the larger freshwater input alone (yellow region; $\sim \delta h_{melt}$), (2) the concentration of the freshwater closer to the surface alone (purple region; $\sim \delta D$), and (3) the contribution of both factors coupled together (green region; $\sim \delta h_{melt} \delta D$) using equations (19) and (20). The yellow region provides a rough estimate of the change in stratification that would occur if the relatively large amount of freshwater input indicated by 2006-2012 ITP data is stored within the relatively deep mixed layer measured by 1975 AIDJEX data (i.e., if $\delta D = 0$ in eqs. (19) and (20)). Similarly, the purple region provides a rough estimate of the change in stratification that would occur if the relatively small amount of freshwater input indicated by 1975 AIDJEX data is stored within the relatively shallow mixed layer measured by 2006-2012 ITP data (i.e., if $\delta \Phi = 0$ in eqs. (19),(20)).

Overall, the changes to the vertical mixing (δD), the freshwater input ($\delta \Phi$), and the coupled contribution ($\delta \Phi \delta D$) have similar roles in explaining the larger magnitudes of $|\mathbb{S}|$ and $|\mathbb{W}|$ in 2006-2012 when compared with 1975. This implies that the concentration of freshwater closer to the surface in recent years has a similar impact on upper-ocean stratification to that caused by a larger amount of seasonal freshwater input. The seasonality of the two factors confirms our findings from Figure 9: The concentration of freshwater closer to the surface (purple region) is mainly important in June–August, while the larger amount of freshwater input and the coupled term (yellow and green regions) are mainly important in August–September. This result is also consistent with the the largest differences in h_{melt} between the two time periods occurring toward the end of the melt season (Fig. 10a).

5. Discussion

In June to mid-August, what mechanisms cause the reduced mixing and stronger stratification in 2006-2012 in response to the same amount of freshwater input as in 1975? Here, we discuss several factors that could explain these differences.

One possibility is that lateral processes are more prominent under the more mobile ice cover in recent years and cause complicated relationships between freshwater input, vertical mixing, and stratification (Randelhoff et al. 2017; Meneghello et al. 2021) or establish fronts that act to limit the effects of wind-driven vertical mixing via submesoscale instabilities (Timmermans and Winsor 2013). A second possibility is that wind-driven momentum transfer has changed in response to changing sea ice conditions. For example, the perennial sea ice cover in 1975 was thicker and associated with more ice keels that extended deeper into the ocean than recent ice keels associated with thinner sea ice cover (Wadhams 2012). This effect can cause the wind-driven momentum transfer to decrease in regions that transitioned from multi-year to first-year ice (McPhee 2012; Martin et al. 2014, 2016; Tsamados et al. 2014). A third possibility is that the shallower and more stably stratified winter halocline in 2006-2012 inhibited mixed-layer deepening to the levels seen in 1975 (Fig. 3; Toole et al. (2010); Peralta-Ferriz and Woodgate (2015)). Each of these mechanisms would create a positive feedback scenario in which the same amount of melt water is concentrated closer to the surface toward the beginning of spring, setting up a more stable seasonal halocline that further inhibits vertical mixing of meltwater, and further stablizes the seasonal halocline.

Another possibility is that changes to the sea ice conditions impact melt-pond drainage, which is associated with halocline formation in early summer (Gallaher et al. 2016). Unfortunately, both the ITPs and AIDJEX measurements begin at an average of ∼6–7 m depth and, therefore, do not capture important variations to the freshwater content near the surface. This surface data gap can cause mixed-layer depths to be biased too deep (Toole et al. 2010), can cause the timing of the mixed-layer shoaling to be biased several weeks too late (Gallaher et al. 2017), and can cause uncertainties in the seasonal freshwater storage. Considering results from Proshutinsky et al. (2009), we estimate that this error could cause h_{melt} to be underestimated by approximately 0.2 m during the summer months (see SI for details). More uncertainties arise because we lack measurements of the sea ice draft (Z_{ice}) for the vertical bounds of our calculations. For example, we find that $\pm$ 1 m changes to Z_{ice} result in approximately $\pm$ 0.1 m of equivalent ice melt by the end of the melt season. Overall, a clear answer to this question will require shallow, near-ice hydrographic or sea ice mass balance measurements in tandem with models to disentangle the sensitivity of vertical mixing to lateral processes, ice-ocean momentum exchange, and pre-melt conditions.

6. Summary

The rapid and continuing change of summer sea ice cover in the Canada Basin has led to a fresher and more stratified upper ocean that has been primarily attributed to more freshwater input from sea ice melt, river-run off, and Ekman convergence of fresh surface waters within the Beaufort Gyre (e.g., McPhee et al. 1998; Macdonald et al. 1999; Yamamoto-Kawai et al. 2009; Jackson et al. 2010; McLaughlin and Carmack 2010; Steele et al. 2011; Peralta-Ferriz and Woodgate 2015;

Carmack et al. 2015). The results presented here indicate that decadal changes to ice-ocean dynamics have a similar impact on the changing seasonal halocline as changes to the freshwater input.

We compared the seasonal evolution of the upper ocean below sea ice in 1975 and 2006-2012, using data collected from the AIDJEX ice camps and ITPs (Fig. 1; Section 2). We interpret differences between the two time periods using a one-dimensional bulk model that allows for the separation of changes in terms of seasonal freshwater input and vertical mixing (Section 3). While upper-ocean dynamics are significantly influenced by spatial and year-to-year variability (Fig. 1; e.g., Yamamoto-Kawai et al. 2009; Peralta-Ferriz and Woodgate 2015; Perovich and Richter-Menge 2015; Proshutinsky et al. 2019; Cole and Stadler 2019), we find that differences between the ITP and AIDJEX datasets yield results that are consistent with decadal trends in the Canada Basin reported by previous studies (Peralta-Ferriz and Woodgate (2015); Section 4a).

By examining the relationships between bulk estimates of the freshwater input (h_{melt}), vertical mixing (D), and stratification ($\mathbb{S}$,$\mathbb{W}$), we found that two separate factors have a similar impact on creating the stronger stratification in 2006-2012 when compared with 1975: larger freshwater input and less vertical mixing (Figs. 8, 9, 10). These results stem from the finding that profiles with the same freshwater input are often associated with less vertical mixing and a more stratified upper-ocean in 2006-2012 than in 1975, particularly in June–July (Fig. 8). In these cases, the stronger stratification in 2006-2012 than in 1975 appears to be unrelated to seasonal freshwater surface fluxes. These results indicate that ice-ocean dynamics, rather than freshwater input alone, play a crucial role in explaining decadal changes to the seasonal halocline in the Canada Basin.

Acknowledgments. The AIDJEX data used in this study can be found at http://lwbin-datahub.ad.umanitoba.ca/dataset/aidjex. The Ice-Tethered Profiler data were collected and made available by the Ice-Tethered Profiler Program based at the Woods Hole Oceanographic Institution (http://www.whoi.edu/itp). All sea ice concentration data created or used during this study are openly available from the NASA National Snow and Ice Data Center Distributed Active Archive Center at https://doi.org/10.5067/8GQ8LZQVL0VL as cited in (Cavalieri et al. 1996).

ER was supported by the National Sciences and Engineering Research Council of Canada (NSERC) PDF award, the Chateaubriand Fellowship of the Office for Science and Technology of the Embassy of France in the United States, and the US National Science Foundation (NSF) Graduate Research Fellowship. ER and JS were supported by the NSERC Canada-150 Chair. STG was supported by the US NSF (Awards PLR-1425989 and OPP-1936222) and by the US Department of Energy (DOE) (Award DE-SC0020073). This work is a contribution to the NSERC - Discovery Grant and the NSF Office of Polar Program grant # 1504023 awarded to LBT. RG was supported by the NSERC Canada Discovery Grant program. RF acknowledges funding from NSERC Canada through a CGS-D award and the US DOE (Grant DE-SC001940).

References

Brown, K. A., J. M. Holding, and E. C. Carmack, 2020: Understanding regional and seasonal variability is key to gaining a pan-Arctic Perspective on Arctic Ocean freshening. *Frontiers Mar. Sci*, **7**, 606, doi:10.3389/fmars.2020.00606.

Carmack, E., and Coauthors, 2015: Towards quantifying the increasing role of oceanic heat in sea ice loss in the new Arctic. *Bulletin of the American Meteorological Society*, doi:10.1175/BAMS-D-13-00177.1.

Carmack, E. C., and Coauthors, 2016: Freshwater and its role in the Arctic Marine System: Sources, disposition, storage, export, and physical and biogeochemical consequences in the

Arctic and global oceans. *Journal of Geophysical Research: Biogeosciences*, **121**, 675–717, doi:10.1002/2015JG003140.

Cavalieri, D., C. L. Parkinson, P. Gloersen, and H. J. Zwally, 1996: Sea Ice Concentrations from SMMR and DMSP SSMI/I-SSMIS Passive Microwave Data, Version1. *Natl. Snow and Ice Data Cent., Boulder, Colo.*, (Updated 2015.) https://nsidc.org/data/nsidc-0051.

Cole, S. T., and J. Stadler, 2019: Deepening of the winter mixed layer in the Canada Basin, Arctic Ocean over 2006-2017. *Journal of Geophysical Research: Oceans*, doi:10.1029/2019JC014940.

Davis, P. E. D., C. Lique, H. L. Johnson, and J. D. Guthrie, 2016: Competing effects of elevated vertical mixing and increased freshwater input on the stratification and sea ice cover in a changing Arctic Ocean. *Journal of Physical Oceanography*, doi:10.1175/JPO-D-15-0174.1.

Gallaher, S., T. Stanton, W. Shaw, S.-H. Kang, J.-H. Kim, and K.-H. Cho, 2017: Field observations and results of a 1-D boundary layer model for developing near-surface temperature maxima in the Western Arctic. *Elementa*, **5**, 1–21, doi:10.1525/elementa.195.

Gallaher, S. G., T. P. Stanton, W. J. Shaw, S. T. Cole, J. M. Toole, J. P. Wilkinson, T. Maksym, and B. Hwang, 2016: Evolution of a Canada Basin ice-ocean boundary layer and mixed layer across a developing thermodynamically forced marginal ice zone. *Journal of Geophysical Research: Oceans*, **121**, 6223–6250, doi:10.1002/2016JC011778.

Galley, R. J., B. G. T. Else, S. J. Prinsberg, D. Babb, and D. G. Barber, 2013: Sea ice concentration, extent, age, motion and thickness in regions of proposed offshore oil and gas development near the Mackenzie Delta – Canadian Beaufort Sea. *Arctic*, doi:10.1029/2018MS001291.

Gudkovich, Z. M., 1961: Relation of the ice drift in the Arctic Basin to ice conditions in Soviet Arctic seas (in Russian). *Tr. Okeanogr. Kom. Akad.*, 11,14–21.

Hunkins, K., and J. A. Whitehead, 1992: Laboratory simulation of exchange through Fram Strait. *Journal of Geophysical Research*, **97(C7)**, 11,299–11,322, doi:10.1029/92JC00735.

Hutchings, J. K., and M. K. Faber, 2018: Sea-ice morphology change in the Canada Basin summer: 2006–2015 ship observations compared to observations from the 1960s to the early 1990s. *Frontiers in Earth Science*, **6**, 2006–2015, doi:10.3389/feart.2018.00123.

Jackson, J. M., E. C. Carmack, F. A. McLaughlin, S. E. Allen, and R. G. Ingram, 2010: Identification, characterization, and change of the near-surface temperature maximum in the Canada Basin, 1993-2008. *Journal of Geophysical Research: Oceans*, **115**, 1–16, doi:10.1029/2009JC005265.

Kern, S., A. Rösel, L. Toudal Pedersen, N. Ivanova, R. Saldo, and R. Tage Tonboe, 2016: The impact of melt ponds on summertime microwave brightness temperatures and sea-ice concentrations. *Cryosphere*, **10**, 2217–2239, doi:10.5194/tc-10-2217-2016.

Kraus, E. B., and J. S. Turner, 1967: A one-dimensional model of the seasonal thermocline II. The general theory and its consequences. *Tellus*, **19 (1)**, 98–106, doi:10.3402/tellusa.v19i1.9753.

Krishfield, R., J. Toole, A. Proshutinsky, and M. L. Timmermans, 2008: Automated ice-tethered profilers for seawater observations under pack ice in all seasons. *Journal of Atmospheric and Oceanic Technology*, **25 (11)**, 2091–2105, doi:10.1175/2008JTECHO587.1.

Kwok, R., 2018: Arctic sea ice thickness, volume, and multiyear ice coverage: Losses and coupled variability (1958-2018). *Environmental Research Letters*, **13**, doi:10.1088/1748-9326/aae3ec.

Kwok, R., and D. A. Rothrock, 2009: Decline in Arctic sea ice thickness from submarine and ICESat records: 1958-2008. *Geophysical Research Letters*, **36**, 1–5, doi:10.1029/2009GL039035.

Kwok, R., G. Spreen, and S. Pang, 2013: Arctic sea ice circulation and drift speed: Decadal trends and ocean currents. *Journal of Geophysical Research: Oceans*, **118 (5)**, 2408–2425, doi:10.1002/jgrc.20191.

Lemke, P., 1987: A coupled one-dimensional sea ice-ocean model. *Journal of Geophysical Research*, **92**, 164–172.

Lemke, P., and T. O. Manley, 1984: The seasonal variation of the mixed layer and the pycnocline under polar sea ice. *Journal of Geophysical Research*, **89**, 6494, doi:10.1029/JC089iC04p06494.

Lique, C., 2015: Ocean science: Arctic sea ice heated from below. *Nature Geoscience*, 1–2, doi:10.1038/ngeo2357.

Lorenz, E., 1955: Available potential energy and the maintenance of the general circulation. *Tellus*, **7 (2)**, 157–167, doi:10.3402/tellusa.v7i2.8796.

Macdonald, R. W., E. C. Carmack, F. A. McLaughlin, K. K. Falkner, and J. H. Swift, 1999: Connections among ice, runoff and atmospheric forcing in the Beaufort Gyre. *Geophysical Research Letters*, **26 (15)**, 2223–2226, doi:10.1029/1999GL900508.

Martin, T., M. Steele, and J. Zhang, 2014: Seasonality and long-term trend of Arctic Ocean surface stress in a model. *Journal of Geophysical Research: Oceans*, **119**, 1723–1738, doi:10.1002/2013JC009425.

Martin, T., M. Tsamados, D. Schroeder, and D. L. Feltham, 2016: The impact of variable sea ice roughness on changes in Arctic Ocean surface stress: A model study. *Journal of Geophysical Research: Oceans*, **121**, 1931–1952, doi:10.1002/2015JC011186.

Martinson, D. G., 1990: Evolution of the Southern Ocean winter mixed layer and sea ice: Open ocean deepwater formation and ventilation. *Journal of Geophysical Research*, **95 (C7)**, 11 641, doi:10.1029/JC095iC07p11641.

Martinson, D. G., and R. Iannuzzi, 1998: Antarctic ocean-ice interactions: Implication from ocean bulk property distributions in the Weddell Gyre. *Antarctic sea ice: Physical processes, interactions and variability, Antarctic Research Series*, **74**, 243–271, doi:10.1029/AR074p0243.

Maykut, G. A., and M. G. McPhee, 1995: Solar heating of the Arctic mixed layer. *Journal of Geophysical Research*, **100**, 24 691, doi:10.1029/95JC02554.

McLaughlin, F., E. Carmack, A. Proshutinsky, R. Krishfield, C. Guay, M. Yamamoto-Kawai, J. Jackson, and B. Williams, 2011: The rapid response of the Canada Basin to climate forcing. *Oceanography*, **24**, 136–145, doi:10.5670/oceanog.2011.66.

McLaughlin, F. A., and E. C. Carmack, 2010: Deepening of the nutricline and chlorophyll maximum in the Canada Basin interior, 2003-2009. *Geophysical Research Letters*, **37 (24)**, 1–5, doi:10.1029/2010GL045459.

McPhee, M. G., 2012: Advances in understanding ice – ocean stress during and since AIDJEX. *Cold Regions Science and Technology*, **76-77**, 24–36, doi:10.1016/j.coldregions.2011.05.001.

McPhee, M. G., and J. D. Smith, 1976: Measurements of the turbulent boundary layer under pack ice. *Journal of Physical Oceanography*, **6**, 696–711, doi:10.1175/1520-0485(1976)006⟨0696:MOTTBL⟩2.0.CO;2.

McPhee, M. G., T. P. Stanton, J. H. Morison, and D. G. Martinson, 1998: Freshening of the upper ocean in the Arctic: Is perennial sea ice disappearing? *Geophysical Research Letters*, **25**, 1729, doi:10.1029/98GL00933.

Meneghello, G., J. Marshall, C. Lique, P. E. Isachsen, E. Doddridge, J. M. Campin, H. Regan, and C. Talandier, 2021: Genesis and decay of mesoscale baroclinic eddies in the seasonally ice-covered interior arctic ocean. *Journal of Physical Oceanography*, **51 (1)**, 115–129, doi: 10.1175/JPO-D-20-0054.1.

Meneghello, G., J. Marshall, M. L. Timmermans, and J. Scott, 2018: Observations of seasonal upwelling and downwelling in the Beaufort Sea mediated by sea ice. *Journal of Physical Oceanography*, **48 (4)**, 795–805, doi:10.1175/JPO-D-17-0188.1.

Morison, J., and J. D. Smith, 1981: Seasonal variations in the upper Arctic Ocean as observed at T-3. *Geophysical Research Letters*, **8**, 753–756, doi:10.1029/GL008i007p00753.

Newton, B., L. B. Tremblay, M. A. Cane, and P. Schlosser, 2006: A simple model of the Arctic Ocean response to annular atmospheric modes. *Journal of Geophysical Research: Oceans*, **111 (9)**, 1–13, doi:10.1029/2004JC002622.

Nummelin, A., C. Li, and L. H. Smedsrud, 2015: Response of Arctic Ocean stratification to changing river runoff in a column model. *Journal of Geophysical Research C: Oceans*, **120 (4)**, 2655–2675, doi:10.1002/2014JC010571.

Parkinson, C. L., J. C. Comiso, H. J. Zwally, W. N. Meier, and J. Stroeve, 2004: Nimbus-5 ESMR Polar Gridded Sea Ice Concentrations, Version 1. *Natl. Snow and Ice Data Cent., Boulder, Colo.*, (Updated 2019.) https://nsidc.org/data/nsidc-0009.

Peralta-Ferriz, C., and R. A. Woodgate, 2015: Seasonal and interannual variability of pan-Arctic surface mixed layer properties from 1979 to 2012 from hydrographic data, and the dominance of stratification for multiyear mixed layer depth shoaling. *Progress in Oceanography*, **134**, 19–53, doi:10.1016/j.pocean.2014.12.005.

Perovich, D., 2011: The Changing Arctic Sea Ice Cover. *Oceanography*, **24 (3)**, 162–173, doi: doi.org/10.5670/oceanog.2011.68.

Perovich, D. K., and J. A. Richter-Menge, 2015: Regional variability in sea ice melt in a changing Arctic. *Phil.Trans.R.Soc.A 373:*, **373**, doi:10.1098.

Petty, A. a., D. L. Feltham, and P. R. Holland, 2013: Impact of atmospheric forcing on Antarctic continental shelf water masses. *Journal of Physical Oceanography*, **43 (5)**, 920–940, doi:10.1175/JPO-D-12-0172.1.

Polyakov, I. V., and Coauthors, 2020: Borealization of the Arctic Ocean in response to anomalous advection From sub-Arctic seas. *Frontiers in Marine Science*, **7**, 1–81, doi:10.3389/fmars.2020.00491.

Proshutinsky, A., and Coauthors, 2009: Beaufort Gyre freshwater reservoir: State and variability from observations. *Journal of Geophysical Research*, **114**, doi:10.1029/2008JC005104.

Proshutinsky, A., and Coauthors, 2019: Analysis of the Beaufort Gyre freshwater content in 2003–2018. *Journal of Geophysical Research: Oceans*, **124**, 9658–9689, doi:10.1029/2019JC015281.

Rampal, P., J. Weiss, and D. Marsan, 2009: Positive trend in the mean speed and deformation rate of Arctic sea ice, 1979-2007. *Journal of Geophysical Research: Oceans*, **114 (5)**, 1–14, doi:10.1029/2008JC005066.

Randelhoff, A., I. Fer, and A. Sundfjord, 2017: Turbulent upper-ocean mixing affected by meltwater layers during Arctic summer. *Journal of Physical Oceanography*, **47 (4)**, 835–853, doi:10.1175/jpo-d-16-0200.1.

Reed, R. J., and B. A. Kunkel, 1960: The Arctic circulation in summer. *Journal of Meteorology*, **17**, 489–506, doi:10.1175/1520-0469(1960)017⟨0489:TACIS⟩2.0.CO;2.

Schauer, U., and M. Losch, 2019: Freshwater in the ocean is not a useful parameter in climate research. *Journal of Physical Oceanography*, **49 (9)**, 2309–2321, doi:10.1175/JPO-D-19-0102.1.

Schweiger, A., R. Lindsay, J. Zhang, M. Steele, and H. Stern, 2011: Uncertainty in modeled Arctic sea ice volume. *Journal of Geophysical Research*.

Simpson, J. H., C. M. Allen, and N. C. G. Morris, 1978: Fronts on the continental shelf. *Journal of Geophysical Research*, **83 (C9)**, 4607, doi:10.1029/jc083ic09p04607.

Simpson, J. H., and J. R. Hunter, 1974: Fronts in the Irish Sea. *Nature*, **250 (5465)**, 404–406, doi:10.1038/250404a0.

Steele, M., W. Ermold, and J. Zhang, 2011: Modeling the formation and fate of the near-surface temperature maximum in the Canadian Basin of the Arctic Ocean. *Journal of Geophysical Research*, **116**, C11 015, doi:10.1029/2010JC006803.

Stroeve, J., and D. Notz, 2018: Changing state of Arctic sea ice across all seasons. *Environmental Research Letters*, **13**, doi:10.1088/1748-9326/aade56.

Stroeve, J. C., T. Markus, L. Boisvert, J. Miller, and A. Barret, ????: Changes in Arctic melt season and implications for sea ice loss. *Geophysical Research Letters*, 1216–1225, doi:10.1002/2013GL058951.

Timmermans, M., and J. Marshall, 2020: Understanding Arctic Ocean circulation: A review of ocean dynamics in a changing climate. *Journal of Geophysical Research: Oceans*, **125**, 1–35, doi:10.1029/2018jc014378.

Timmermans, M. L., and P. Winsor, 2013: Scales of horizontal density structure in the Chukchi Sea surface layer. *Continental Shelf Research*, **52**, 39–45, doi:10.1016/j.csr.2012.10.015.

Tivy, A., S. E. Howell, B. Alt, S. McCourt, R. Chagnon, G. Crocker, T. Carrieres, and J. J. Yackel, 2011: Trends and variability in summer sea ice cover in the Canadian Arctic based on the Canadian Ice Service Digital Archive, 1960-2008 and 1968-2008. *Journal of Geophysical Research: Oceans*, **116**, doi:10.1029/2009JC005855.

Toole, J. M., M. L. Timmermans, D. K. Perovich, R. A. Krishfield, A. Proshutinsky, and J. A. Richter-Menge, 2010: Influences of the ocean surface mixed layer and thermohaline stratification on Arctic Sea ice in the central Canada Basin. *Journal of Geophysical Research: Oceans*, **115**, 1–14, doi:10.1029/2009JC005660.

Tsamados, M., D. Feltham, A. Petty, D. Schroder, and D. Flocco, 2015: Processes controlling surface, bottom and lateral melt of Arctic sea ice in a state of the art sea ice model . *Philosophical Transactions of the Royal Society A*, **17**, 10 302, doi:10.1098/rsta.2014.0167.

Tsamados, M., D. L. Feltham, D. Schroeder, D. Flocco, S. L. Farrell, N. Kurtz, S. W. Laxon, and S. Bacon, 2014: Impact of variable atmospheric and oceanic form drag on simulations of arctic sea ice. *Journal of Physical Oceanography*, **44**, 1329–1353, doi:10.1175/JPO-D-13-0215.1.

Turner, J., 1967: A one-dimensional model of the seasonal thermocline I. A laboratory experiment and its interpretation. *Tellus*, **19 (1)**, 88–97, URL http://onlinelibrary.wiley.com/doi/10.1111/j.2153-3490.1967.tb01461.x/abstract.

Untersteiner, N., A. S. Thorndike, D. A. Rothrock, and K. L. Hunkins, 2007: AIDJEX revisited: A look back at the U.S.-Canadian Arctic Ice Dynamics Joint Experiment 1970-78. *Arctic*, **60**, 327–336, doi:10.14430/arctic233.

Wadhams, P., 2012: New predictions of extreme keel depths and scour frequencies for the Beaufort Sea using ice thickness statistics. *Cold Regions Science and Technology*, **76-77**, 77–82, doi: 10.1016/j.coldregions.2011.12.002.

Yamamoto-Kawai, M., F. A. McLaughlin, E. C. Carmack, S. Nishino, K. Shimada, and N. Kurita, 2009: Surface freshening of the Canada Basin, 2003-2007: River runoff versus sea ice meltwater. *Journal of Geophysical Research: Oceans*, **114**, 2003–2007, doi:10.1029/2008JC005000.

LIST OF TABLES

TABLE 1. List of AIDJEX ice camps and ITPs used in the study.

Ice Camp	Time Period Used
Blue Fox	May 10, 1975 - Sept. 31, 1975
Caribou	May 14, 1975 - Sept. 31, 1975
Snowbird	May 16, 1975 - Sept. 31, 1975
Big Bear	May 1, 1975 - Sept. 31, 1975
ITP	**Time Period Used**
1	May 1, 2006 - Sept. 31, 2006
3	May 1, 2006 - Sept. 10, 2006
4	May 1, 2007 - Aug. 17, 2007
5	May 1, 2007 - Aug. 2, 2007
6	May 1, 2007 - Sept. 31, 2007
8	May 1, 2008 - Sept. 31, 2008
11	May 1, 2009 - July 20, 2009
13	May 1, 2008 - Aug. 8, 2008
18	May 1, 2008 - Sept. 31, 2008
33	May 1, 2010 - Sept. 31, 2010
41	May 1, 2011 - Sept. 31, 2011
41	May 1, 2012 - Sept. 31, 2012
53	May 1, 2012 - Aug. 5, 2012

TABLE 2. List of constants and variable names.

Name	Description	Value
Z_{ice}	ice-ocean interface	3 m
β	haline contraction coefficient	0.81 $kg^2/m^3/g$
ρ_{ice}	sea ice density	900 kg/m^3
S_{ice}	sea ice salinity	5 g/kg
H	see definition for $\mathbb{W}$	33 m
$\mathbb{S}$	seasonal surface freshening	—
$\mathbb{W}$	estimated work to completely mix to depth H	—
h_{melt}	freshwater input in terms of ice melt	—
sFWC	freshwater input in terms of freshwater	—
Φ	measure of freshwater input	—
Z_{fw}	penetration depth of freshwater input	—
D	equivalent mixed-layer depth	—
$\mathbb{S}_{bulk}$	as in $\mathbb{S}$ but for 2-layer system	—
$\mathbb{W}_{bulk}$	as in $\mathbb{W}$ but for 2-layer system	—

LIST OF FIGURES

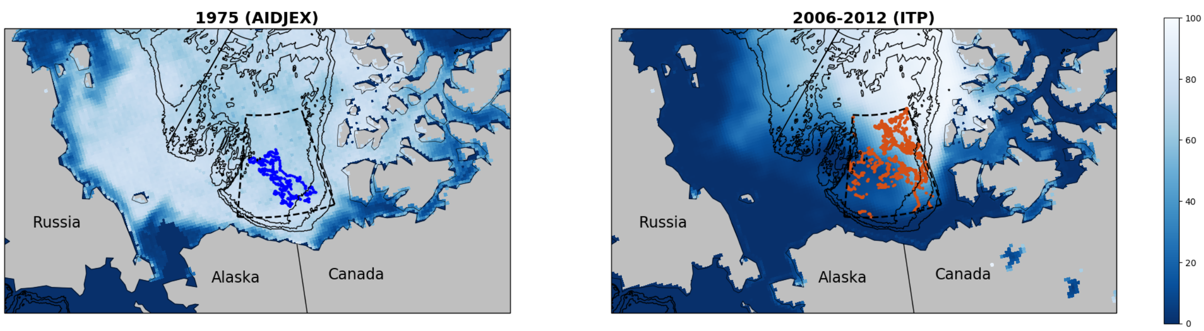

FIG. 1. Map of Canada Basin showing September sea ice concentration and location of ocean observations. (Left) September 1975 mean sea ice concentration and location of measurements from AIDJEX sea ice camps (blue dots) and (right) 2006-2012 September-mean sea ice concentration and location of ITP observations (red dots). Region indicated by dashed-lines shows the Canada Basin, which we define as the region bounded by 72°N, 80°N, 130°W, and 155°W. Solid lines indicate bathymetric contours at 1000 m, 2000 m, and 3000 m. The regional map of September 1975 sea ice concentrations are provided by Nimbus-5 ESMR Polar Gridded Sea Ice Concentrations, Version 1 (Parkinson et al. 2004)

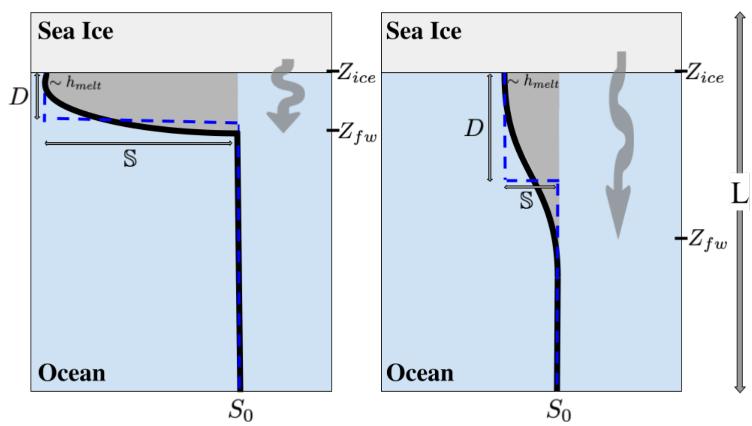

FIG. 2. Schematic of one-dimension ice-ocean model, showing an illustration of the salinity profile resulting from ice melt that is concentrated close to the surface (left) and an example where the a similar amount of ice melt is mixed over a larger depth range (right). D, Z_{ice}, and Z_{fw} are negative values that indicate depths. S_0 and $\mathbb{S}$ indicate the initial salinity and surface freshening, respectively. Gray shading is directly related to the equivalent sea ice melt (h_{melt}).

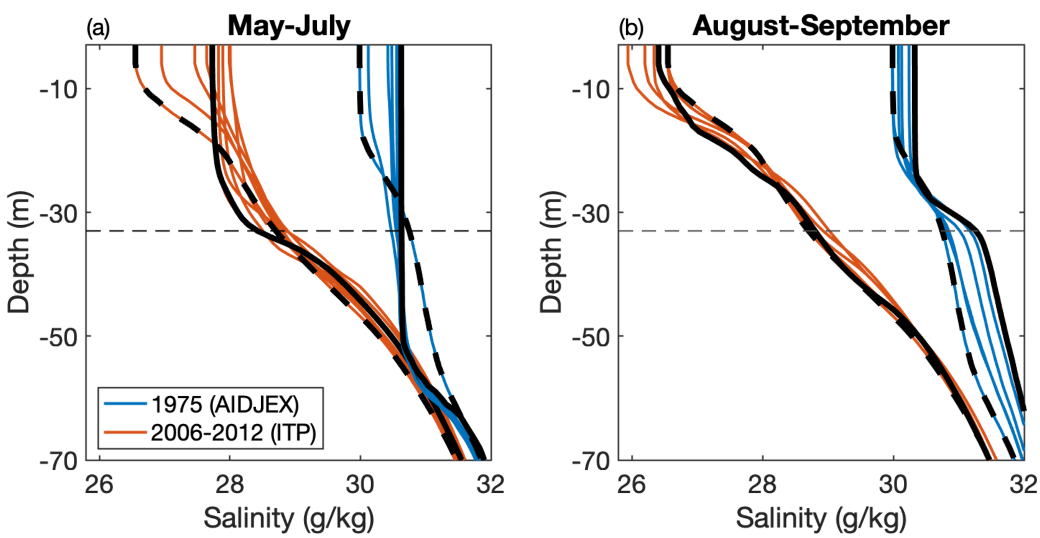

FIG. 3. 10-day mean profiles during (a) May-July and (b) August-September in 1975 (blue) and 2006-2012 (red). Solid black lines indicate 10-day mean profiles from (a) the beginning of May and (b) the end of September. Dashed lines indicate common 10-day mean profile that marks the end of July and the beginning of August, (July 30 - August 8) and are the same in panels a and b. Horizontal dashed lines indicate $H = 33$m. Note that changes to the average mixed-layer salinity near the beginning of the melt season are small compared to the spatial variability.

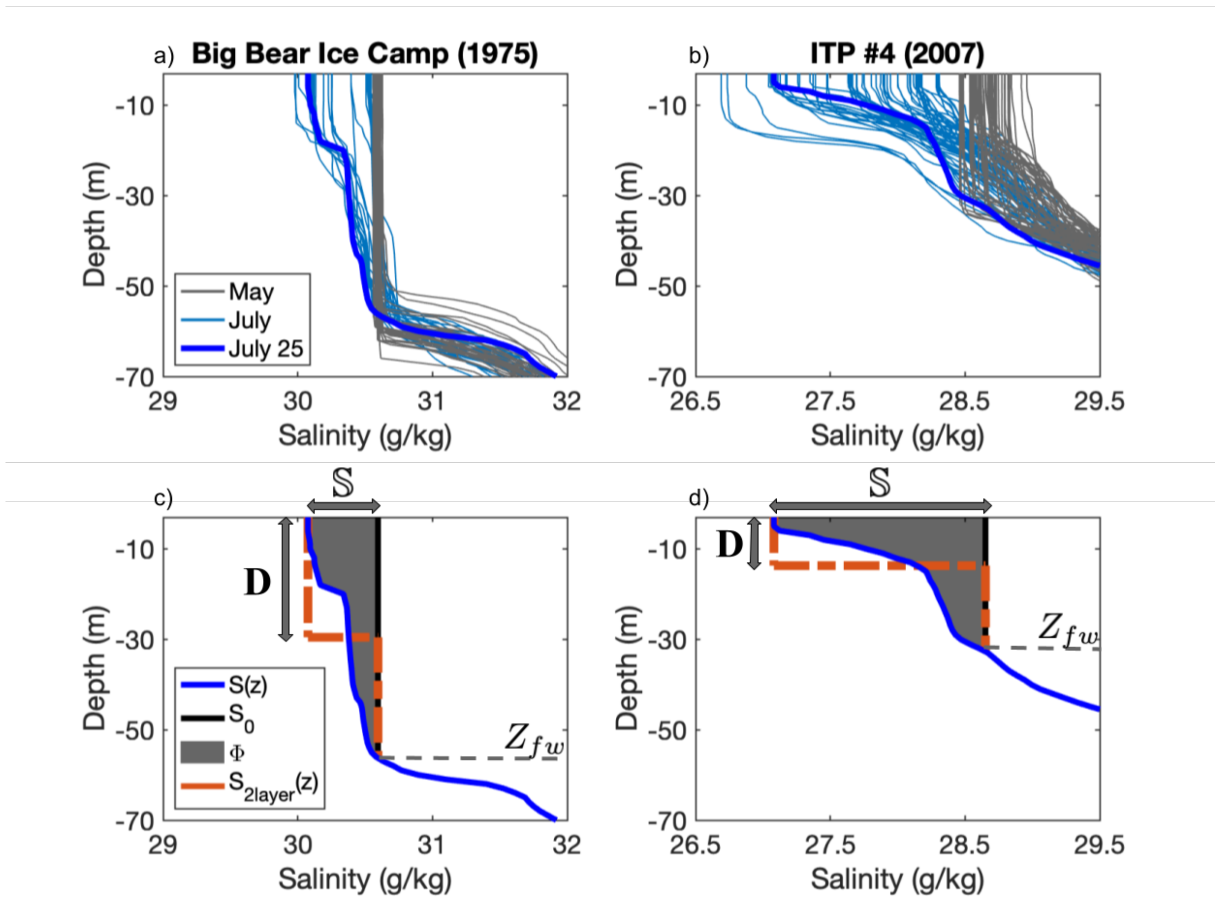

FIG. 4. Observed salinity profiles using data from (left) AIDJEX Big Bear ice camp in 1975 and (right) ITP #4 in 2007 to illustrate the methods used to estimate metrics derived in Section 3. (a-b) All observed salinity profiles measured during the month of May (gray lines) and July (blue lines), with July 25th highlighted in dark blue ($S(z)$). (c-d) Black line indicates May-average surface salinity (S_0), area covered by gray shading is the same as Φ associated with the observed July 25 profile. The associated 2-layer salinity profile (red dashed lines, $S_{bulk}(z)$), which give the surface freshening $\mathbb{S}$ and equivalent mixed-layer depth D is shown in red. Blue lines are the same in panels (a,c) and (b,d).

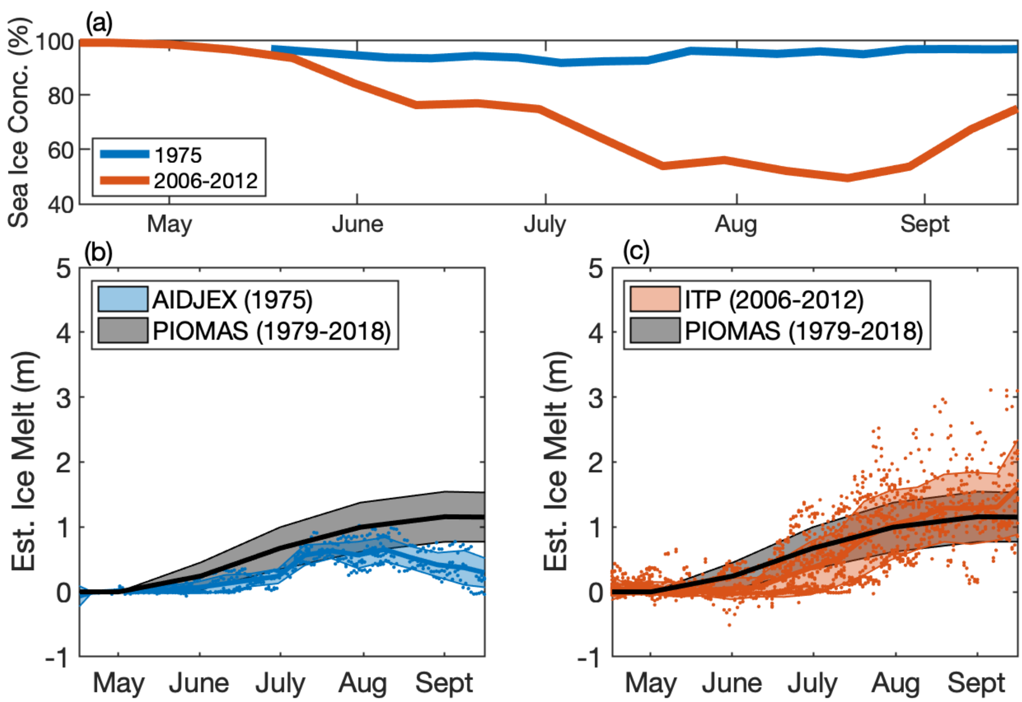

FIG. 5. (a) Sea ice concentration and (b-c) estimated freshwater input in terms of sea ice thickness changes in 1975 (blue), 2006-2012 (red). PIOMAS data provide a climatological monthly effective sea ice thickness change relative to May of each year between 1979-2018 (black). Blue and red lines indicate 5-day mean, black lines indicate monthly mean, and shadings indicate one standard deviation.

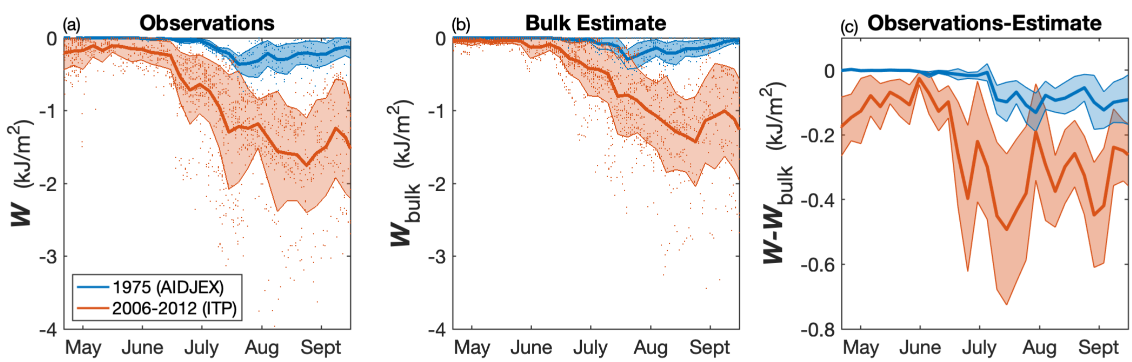

FIG. 6. Comparison of observations to bulk estimates using $\mathbb{W}$ (left), $\mathbb{W}_{bulk}$ (center), and $\mathbb{W} - \mathbb{W}_{bulk}$ (right) in 1975 (blue) and 2006-2012 (red). $\mathbb{W}$ and $\mathbb{W}_{bulk}$ are computed for each observed profile. Lines indicate 5-day means and shading indicates one standard deviation (left, center panels) or standard error (right panels).

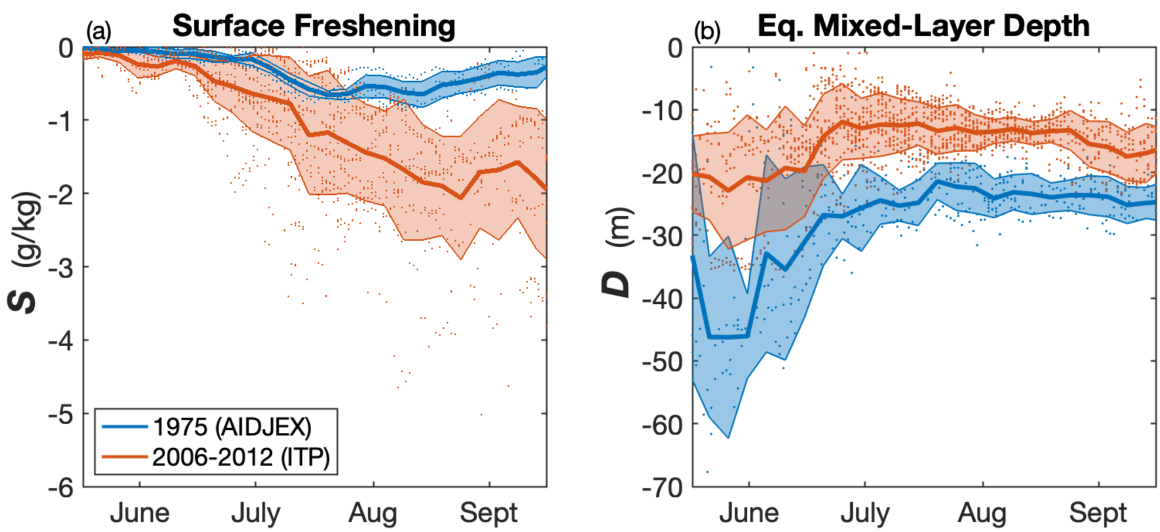

FIG. 7. (a) Surface freshening ($\mathbb{S}$) and (b) equivalent mixed-layer depth (D) in 1975 (blue) and 2006-2012 (red). $\mathbb{S}$ and D are computed for each observed profile. Lines indicate 5-day means and shading indicates one standard deviation.

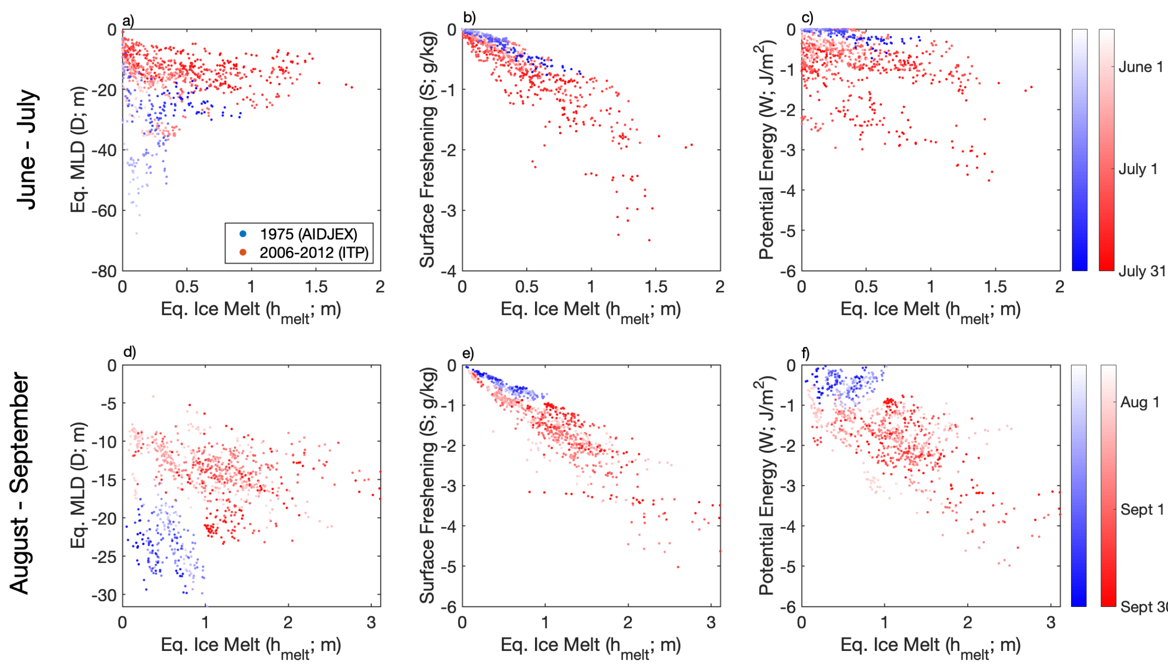

FIG. 8. Relationships between equivalent sea ice melt (h_{melt}) and (a,d) equivalent mixed-layer depth (D), (b,e) surface freshening ($\mathbb{S}$), and (c,f) upper-ocean stratification ($\mathbb{W}$) using all profiles in 1975 (blue) and 2006-2012 (red) during June-July (a-c) and August-September (d-f). Shadings indicate date of measurement.

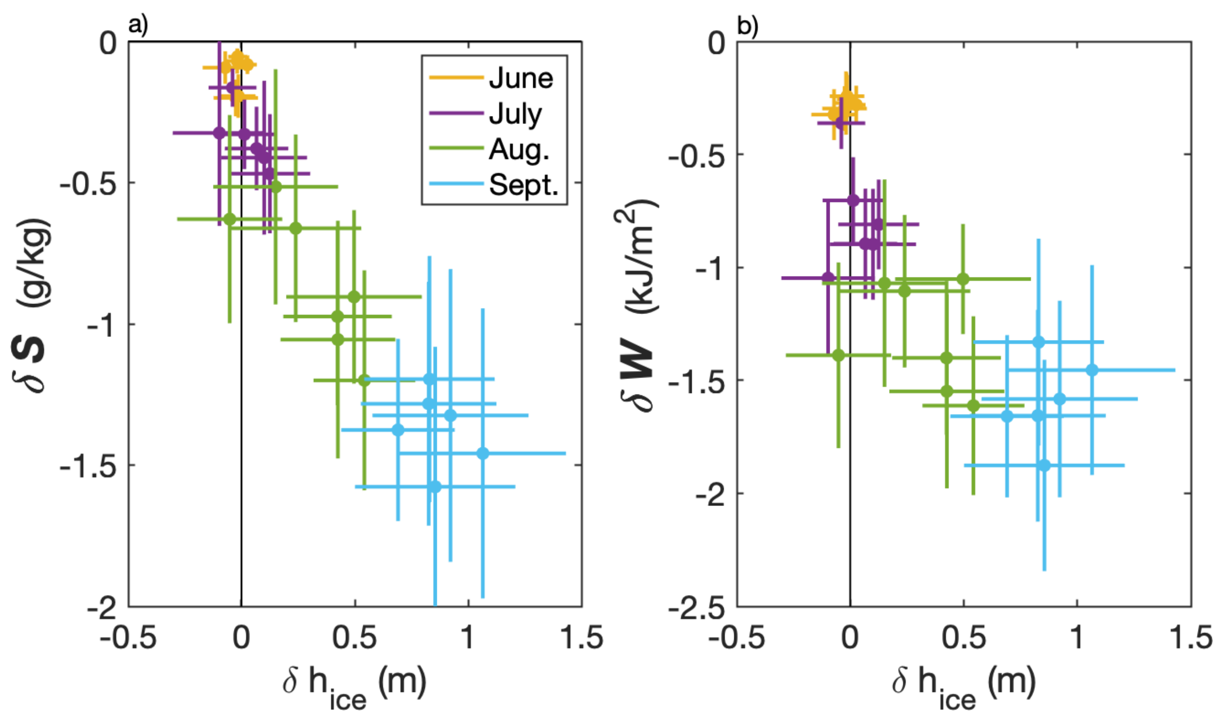

754 FIG. 9. Five-day average differences between 1975 and 2006-2012 using the equivalent ice melt (δh_{melt}), the
755 surface freshening ($\delta\mathbb{S}$), and the potential energy anomaly ($\delta\mathbb{W}$). Colors indicate month and lines indicate one
756 standard error.

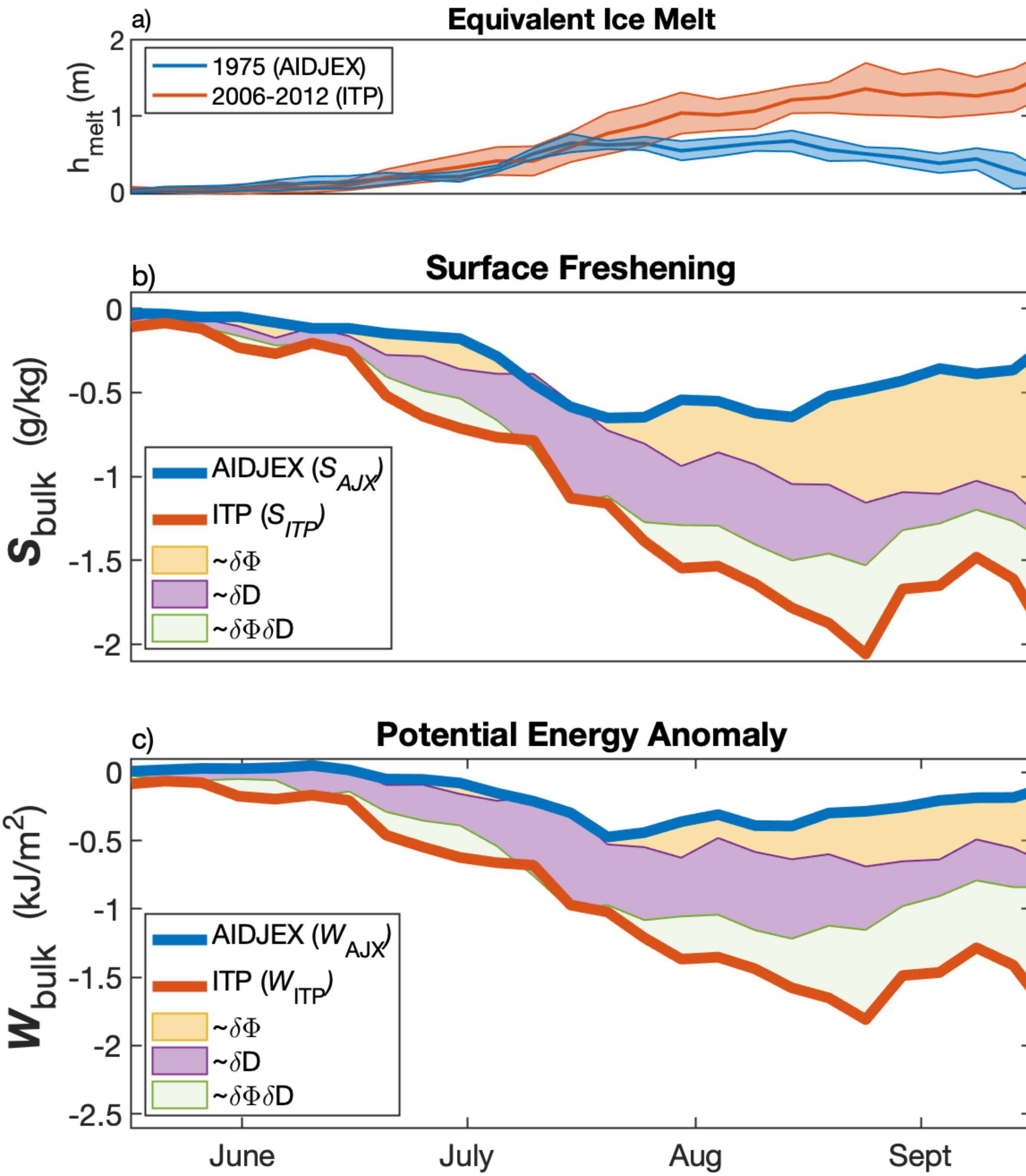

FIG. 10. Five-day mean (a) equivalent ice melt (h_{melt}), (b) surface freshening using the 2-layer estimate ($\mathbb{S}_{bulk}$), and (c) potential energy anomaly using the 2-layer estimate ($\mathbb{W}_{bulk}$) in 1975 (blue) and 2006-2012 (red). (b-c) Colors are associated with three terms that contribute to the difference between 1975 and 2006-2012 ($\delta\mathbb{S}$, $\delta\mathbb{W}$).